AAPT PHYSICS EDUCATION | AMERICAN JOURNAL of PHYSICS

Man-made quantum wells: A new perspective on the finite square-well problem

R. M. Kolbas and N. Holonyak Jr.

Citation: American Journal of Physics **52**, 431 (1984); doi: 10.1119/1.13649
View online: http://dx.doi.org/10.1119/1.13649
View Table of Contents: http://scitation.aip.org/content/aapt/journal/ajp/52/5?ver=pdfcov
Published by the American Association of Physics Teachers

Man-made quantum wells: A new perspective on the finite square-well problem

R. M. Kolbas
Honeywell Corporate Physical Sciences Center, Bloomington, Minnesota 55420

N. Holonyak, Jr.
Department of Electrical Engineering and Materials Research Laboratory, University of Illinois at Urbana-Champaign, Urbana, Illinois 61801

(Received 20 September 1982; accepted for publication 5 August 1983)

The observation of man-made quantum size effects is now possible due to advances in semiconductor technology. Interest in quantum-well heterostructures and superlattices has added a new dimension to both the application and perspective of the traditional discussion of a particle in a box. This paper addresses these new perspectives and presents in an elementary manner the techniques employed to model single and multiple square wells in semiconductors. A brief overview of semiconductor microlayer devices is followed by a discussion of the physics of quantum-well heterostructures. Since the behavior of these structures is described by the finite square well, a simple iterative technique to solve for the bound states of *single* or *multiple* (coupled) square wells is presented. The iterative technique is quite general and powerful, yet the physical ideas and the mathematics are straightforward and simple. Finally, computer simulation is employed to illustrate the interaction between multiple coupled wells; the results are compared with those obtained via the usual Kronig–Penney model.

I. INTRODUCTION

Until recently examples of the quantum-mechanical particle in a box have been limited to naturally occurring systems such as alpha-particle emission from heavy nuclei,[1] the Ramsauer–Townsend effect,[2] or in recent times ultrathin conducting channels in field-effect transistors.[3] Advances in controlling the epitaxial growth of semiconductor heterostructures have made possible the observation of man-made quantum size effects in optical devices. By careful control of III-V crystal growth processes researchers have been able to fabricate a variety of high performance optoelectronic and electronic devices involving confined-particle (quantum) effects. These devices add a new dimension to the traditional view of the classic problem of a particle in a box and its application in studying quantum-well heterostructure devices. The purpose of this paper is to introduce the subject of quantum-well heterostructures and to present in an elementary manner the techniques employed to model these structures via single and multiple square wells. The iterative numerical technique presented (and the solution of bound-state energies) is based on previous work but is considerably more general and yet still is simple.

This paper is organized into five sections. In this section an introduction to ultrathin-layer (quantum-well) semiconductor devices is given. Section II presents background information on the modeling of quantum-well heterostructures. In Sec. III a simple iterative technique to determine the bound-state energies and wave functions of single and multiple finite square wells is presented. In Sec. IV we illustrate the formation of minibands for a large number of identical coupled wells and compare the exact solutions to the Kronig–Penney model. Each section is relatively self-contained so that readers interested primarily in the square-well solutions can proceed directly to Sec. III.

The evolution of semiconductor crystal growth has advanced to the stage where "artificial" materials can be created in the form of ultrathin layers of narrow-band gap adjacent to layers of wideband gap. The optical and electrical properties of these new materials can be quite different from those of bulk crystals. Quantum effects play a very explicit role in determining the new properties.[4,5]

A layer of gallium arsenide (GaAs) less than 200 Å thick sandwiched (epitaxially, i.e., the atoms in registry) between two aluminum gallium arsenide ($Al_xGa_{1-x}As$) confining layers is an example of the type of artificial structure that has been grown in recent years. This sandwiched structure, an $Al_xGa_{1-x}As$–GaAs quantum-well heterostructure (QWH), creates a conduction band (and valence band) potential well, and consequently a set of discrete energy levels can be observed for electrons confined in the thin GaAs layer. If several alternating layers of $Al_xGa_{1-x}As$ and GaAs are grown, then a multiple quantum-well heterostructure can be fabricated. If the number of adjacent wells is very large, the structure is called a superlattice (SL). It is an interesting question: How many coupled wells form a SL? As we shall see later, the answer is not many—maybe less than ten.

Interest in quantum-well heterostructures and superlattices has increased dramatically because of various fundamental properties and the fact that a variety of novel (and useful) optoelectronic and electronic devices are possible based on QWH designs.[4,5] One of the most important aspects of QWH's and SL's is that their unique properties can be "engineered" by controlling the layer thickness, crystal or alloy composition, or doping. To understand how this control is achieved it is necessary to understand the quantum ideas governing these structures. For the case of quantum wells and superlattices in which the layer thicknesses and composition are varied, the QWH or SL problem can be modeled as a particle-in-a-box or a finite square-well potential. (If the crystal doping is varied or if charge transfer occurs from one layer to another, then the potential is no longer a square well and is not considered in this paper.) The challenge in modeling quantum-well heter-

ostructures arises from the large variety of these structures that can be fabricated. The simplest structure is a single finite square well. However, desirable device geometries can include multiple square wells of different well widths and barrier heights. The determination of the bound-state energies of such a complicated system is actually quite easy if some straightforward iterative techniques are applied.

II. QUANTUM-WELL HETEROSTRUCTURES

The physical system of interest here consists of a narrow-band-gap thin layer of GaAs ($L_z < 200$ Å) sandwiched (epitaxially) between two wider-band-gap $Al_x Ga_{1-x} As$ layers as shown in Fig. 1. (The crystal composition x can vary between 0 and 1. As the composition x is increased the band gap (E_g) of the $Al_x Ga_{1-x} As$ increases.[6]) The difference in band gap $\Delta E_g = E_g(\text{AlGaAs}) - E_g(\text{GaAs})$ produces an attractive potential well to electrons in the conduction band ($\Delta E_c = 0.85 \Delta E_g$)[7] and an attractive potential well to holes in the valence band ($\Delta E_v = 0.15 \Delta E_g$)[7] as shown in Fig. 2. (A brief review of solid-state physics terminology is given in the Appendix.)

If an electron from the conduction band of a bulk piece of GaAs recombines with a hole in the valance band, then the energy of the emitted photon is given by $E_p = E_g(\text{GaAs}) = \hbar\omega$. A similar transition (a confined-particle transition) in a GaAs quantum well results in a photon of energy $E_p = E_g(\text{GaAs}) + E_n^{cb} + E_m^{vb}$, where E_n^{cb} is the nth bound-state electron energy in the conduction band and E_m^{vb} is the mth bound-state hole energy in the valance band. That is, the photon released has an energy equal to the sum of the bulk band-gap energy plus the bound-state energies of the electron and hole as shown in Fig. 2. The most probable optical transitions occur when $n = m$ since $n \neq m$ transitions involve wave functions (electrons and holes) which are nearly orthogonal. The luminescence spectrum, or optical emission spectrum, from a quantum well should contain a series of emission lines corresponding to the bound-state energies of the potential well. Spectra of this form are indeed observed as shown in Fig. 3. The various positions of the electron-to-heavy-hole ($e \rightarrow$hh; dark markers, n) and electron-to-light-hole ($e \rightarrow$lh; light markers, n') recombination transitions for the experimental sample are shown on the horizontal axis of Fig. 3. Note that light is emitted (actually stimulated emission) in

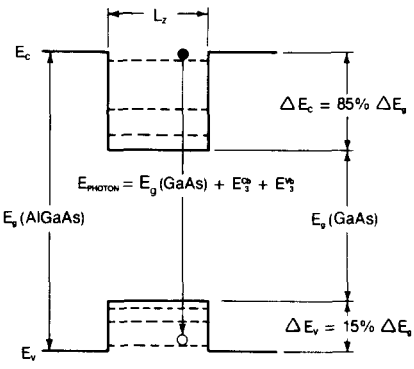

Fig. 2. Square-well potential characteristic of an $Al_x Ga_{1-x} As$–GaAs–$Al_x Ga_{1-x} As$ quantum-well heterostructure. For well thicknesses $L_z < \lambda$ (the carrier de Broglie wavelength) size quantization occurs and results in a series of discrete energy levels given by the bound-state energies of a finite square well. An attractive potential well occurs in both the conduction band and the valence band, giving rise to a series of bound electron states E_n^{cb}, and bound hole states E_m^{vb}. In the valence band there are bound heavy-hole states and bound light-hole states. (Light-hole states not shown.)

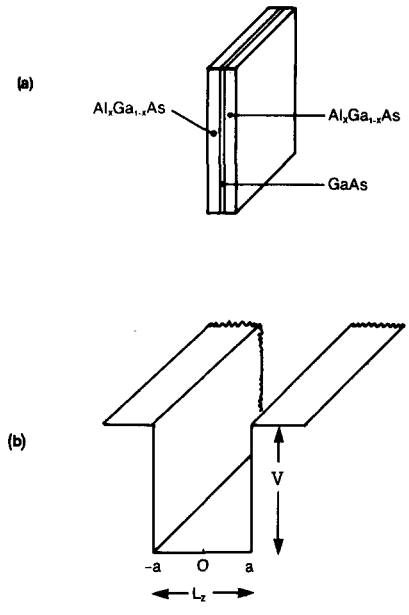

Fig. 1. Schematic representation of an $Al_x Ga_{1-x} As$–GaAs–$Al_x Ga_{1-x} As$ quantum-well heterostructure. (a) An ultrathin ($L_z = 200$ Å) narrow-band-gap GaAs active layer is sandwiched between two thick wider-gap $Al_x Ga_{1-x} As$ layers. (b) Electrons (and holes) are trapped in the thin GaAs layer by a finite square-well potential.

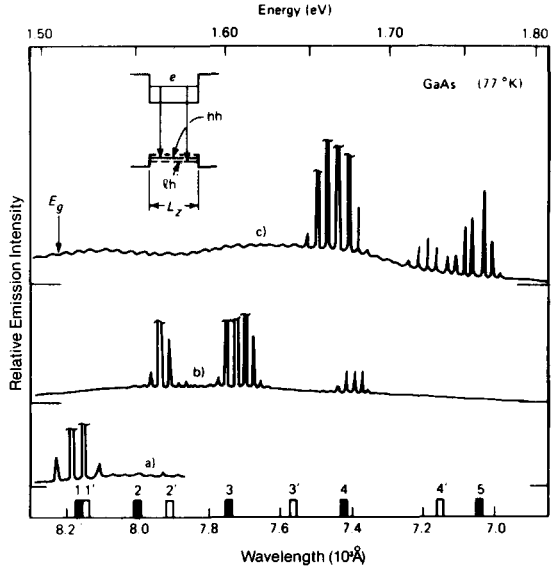

Fig. 3. Stimulated emission (77 K) on confined-particle states of an $Al_x Ga_{1-x} As$–GaAs–$Al_x Ga_{1-x} As$ ($x = 0.6$) quantum-well heterostructure grown by metalorganic chemical vapor deposition. The calculated energies of the confined particle recombination transitions ($L_z = 235$ Å) are indicated on the horizontal axis by heavy ($e \rightarrow$hh, n) and light ($e \rightarrow$lh, n') markers. Notice that laser operation occurs on well-defined, confined-particle transitions as far as the $n = 5$ state or 265 meV above the bulk-crystal GaAs band edge (E_g). The experimental samples [of lateral width (a) 15 μm, (b) 31 μm, and (c) 26 μm] are photopumped (5×10^4 W/cm^2, Ar^+ laser) at various positions on the flat sides of the samples. The fine structure is due to the Fabry–Perot modes of the laser cavity.

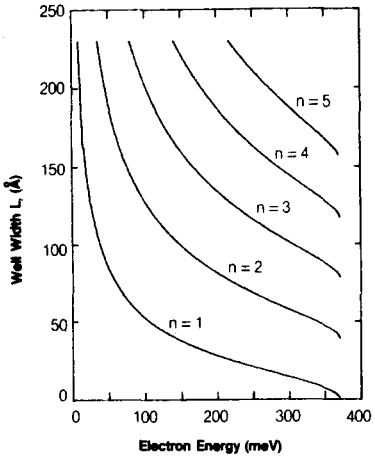

Fig. 4. Electron energies as a function of layer thickness L_z for a thin GaAs layer sandwiched between two $Al_xGa_{1-x}As$ ($x = 0.35$) confining or barrier layers. The depth of the well for the electrons is 371 meV. The hole energies for the same sample are shown in Fig. 5.

well-defined groups of modes near the calculated transition energies. The fine structure which occurs at each quantum state is due to the Fabry–Perot modes of the laser cavity. A detailed description of Fig. 3 and other single/multiple quantum-well laser spectra can be found in Ref 8. In this case the effects of size quantization are quite dramatic and easy to observe. Laser operation hundreds of milli-electron-volts above the GaAs band edge (*visible* red light from GaAs) is unique to quantum-well heterostructures and forms the basis of many important experiments.

The bound-state electron energies (E_n^{cb}) and bound-state hole energies (E_m^{vb}) for an $Al_xGa_{1-x}As$–GaAs–$Al_xGa_{1-x}As$ ($x = 0.35$) quantum well as a function of well width L_z are shown in Figs. 4 and 5, respectively. The room-temperature band gaps of GaAs and $Al_{0.35}Ga_{0.65}As$ are 1.424 and 1.860 eV, respectively.[6] The resulting potential wells in the conduction band and valence band are 0.371 and 0.065 eV. (The curves of Figs. 4 and 5 take into account the difference in effective mass between the GaAs and $Al_xGa_{1-x}As$.) Note the rapid increase in E_n^{cb} (and E_m^{vb}) as the well width L_z is decreased. Note also that each plot terminates at 0.371 eV (or 0.065 eV), which corresponds to the potential well depth. From curves such as these it is possible to calculate the optical transition energies $E_g(\text{GaAs}) + E_n^{cb} + E_n^{vb}$. In the remainder of this section the techniques used to calculate the electron and hole bound-state energies are presented. (An interesting exercise for those who are already familiar with square wells is to explain the origin of the slight downturn of each curve for energies approaching the well depth V.)

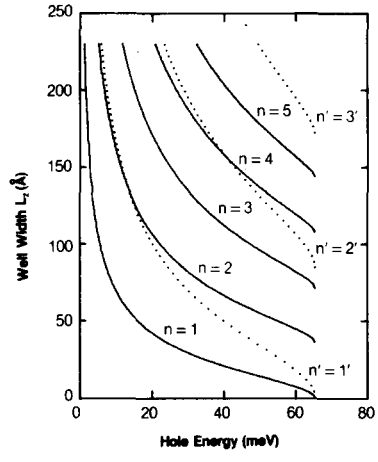

Fig. 5. Heavy- and light-hole (dotted) energies as a function of layer thickness L_z for a GaAs quantum well with $Al_xGa_{1-x}As$ ($x = 0.35$) confining or barrier layers. The depth of the well for holes is 65 meV. From Figs. 4 and 5 the optical transition energies are given by the electron energy + band-gap energy + hole energy, for a specific well width L_z.

We now consider in greater detail the physics of quantum-well heterostructures. Electrons (and holes) trapped in the thin GaAs layer can be considered to be confined in a three-dimensional finite potential well where $L_z \ll L_x, L_y$. If the spacial dimensions are large (e.g., L_x and L_y), then the allowed energies form a continuum and $E = \hbar^2 k^2/2m$, where k can take on many closely spaced values. If one of the spacial dimensions is small (e.g., $L_z <$ carrier de Broglie wavelength), then quantization of the particle motion occurs and $E = \hbar^2 k_z^2/2m$, where k_z is determined by the solutions to the finite square-well problem. The potential in the z direction is shown in Fig. 2.

The formal method of describing the electrons (or holes) in the thin GaAs layer is to write down the appropriate Hamiltonian. Since $L_z \ll L_x, L_y$ for the QWH of interest here (Figs. 1 and 2), to a first approximation the following separation can be made:

$$H_{\text{tot}} = H_{xy} + H_z, \tag{1}$$

where H_{xy} is the single-particle Hamiltonian for a two-dimensional electron gas and H_z is the Hamiltonian for a one-dimensional finite square well. Regardless of our knowledge of Hamiltonian operators, the basic idea is that our three-dimensional system can be conveniently split into a two-dimensional system plus a one-dimensional system. By virtue of the "well-behaved" mathematical character of our Hamilitonian operator and the allowed wave functions, the energy of an electron (or a hole) in the thin GaAs layer is given by the sum of the energies associated with H_z and H_{xy}. These are

$$E(k_x,k_y,k_z) = \frac{\hbar^2 k_z^2}{2m} + \frac{\hbar^2}{2m}(k_x^2 + k_y^2) \tag{2}$$

or

$$E(k_x,k_y,n) = E_n + \frac{\hbar^2}{2m}(k_x^2 + k_y^2), \tag{3}$$

where $E_n = \hbar^2 k_z^2/2m$ is the nth bound state of the potential well. The virtue of this analysis is that a rather overwhelming physical system is reduced to the solution of two relatively simple problems. The first problem is that of a one-dimensional square well, as we have been suggesting all along. The second problem requires a knowledge of the band structure of GaAs. Band-structure information is readily obtained from previous work (e.g., band-gap energy, electron effective mass, etc.).[6]

The dispersion relations (3) describe the electron or hole energies by one discrete quantum number n (k_z discrete) and two continuous quantum numbers k_x and k_y. Many of the unique properties of QWH can be understood by the appropriate inspection/manipulation of Eq. (3). For each confined particle state E_n there is a continuum of k_x and k_y values allowed (called a subband). Each subband is displaced from the band edge by an amount E_n which corre-

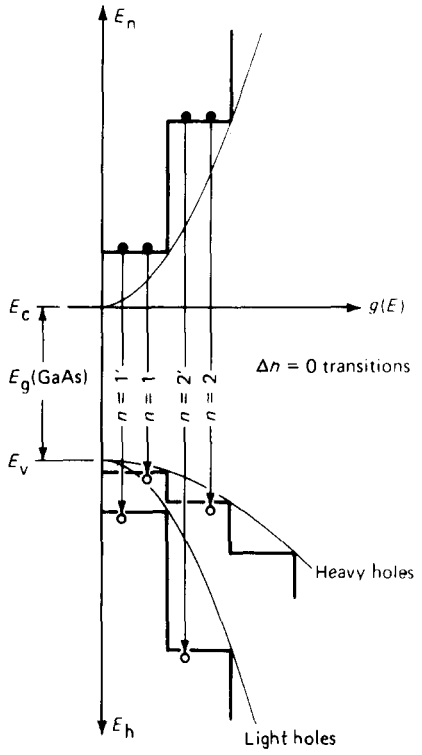

Fig. 6. Plot of increasing electron energy and increasing hole energy (downward) as a function of the density of states for a QWH. The staircase density of states is characteristic of the two-dimensional nature of a quantum well. The smooth parabolic curves correspond to the bulk-crystal density of states. Interband optical transitions ($\Delta n = 0$ selection rule assumed) occur from a bound state in the conduction band E_n^{cb} to a bound state in the valence band E_m^{vb} with $n = m$. Electron transitions can occur to both light- and heavy-hole valence-band states. The energy of the emitted quanta is given by $\hbar\omega = E_g(\text{GaAs}) + E_n^{cb} + E_n^{vb}$. (Note that the *hole* degeneracy of light and heavy holes of bulk GaAs is removed by the small size $L_z < \lambda$.)

sponds to the bound-state (one-dimensional) energies of a finite potential well.

The form of the dispersion relation also determines the form of the density of states function $g(E)$ (number of allowed states/energy interval). A comparison between the density of states for a thick sample (parabola) and QWH (staircase) is shown in Fig. 6. Since many optical and electrical properties depend on $g(E)$ and $d[g(E)]/dE$ the staircase form of $g(E)$ for quantum wells gives rise to unique materials and device characteristics[8] not observed in thick samples.

The origin of the selection rule $E_n^{cb} \rightarrow E_m^{vb}$, $n = m$ ($\Delta n = 0$) for interband transitions (see Fig. 3 and 4) arises from the near orthogonality of the electron and hole wave functions. This is not, however, a strict selection rule.[9]

In summary, we have divided the study of quantum-well heterostructures into two parts to simplify the analysis. The two parts consist of a two-dimensional electron gas with continuous energy states and a one-dimensional square well with discrete bound states. For additional experimental information on quantum-well heterostructures see Refs. 4, 5, and 7–9.

III. NUMERICAL SOLUTION OF MULTIPLE SQUARE WELLS

The bound-state energies of the one-dimensional finite square well are given by the solution of the time-independent Schrödinger equation $H\psi = E\psi$. For the square well of depth V and well width $L_z = 2a$, the Schrödinger equation is given by

$$\frac{-\hbar^2}{2m}\frac{d^2\Psi}{dz^2} = E\Psi,$$

$$\text{for } -a < z < a,\ \Psi(z) = A\sin(\alpha z) + B\cos(\alpha z) \tag{4}$$

and

$$\frac{-\hbar^2}{2m}\frac{d^2\Psi}{dz^2} + V\Psi = E\Psi,$$

$$\text{for } z < -a,\ \Psi(z) = Ce^{\beta z};\ \text{for } z > a,\ \Psi(z) = De^{-\beta z}, \tag{5}$$

where

$$\alpha = (2mE/\hbar^2)^{1/2},\quad \beta = (2m(V-E)/\hbar^2)^{1/2}. \tag{6}$$

These results, of course, appear in many introductory quantum mechanics textbooks. Continuity of the wave function $\psi(z)$ and the first derivative $\psi'(z)$ at the two well boundaries results in two transcendental equations

$$\alpha\tan(\alpha a) = \beta \quad \text{(symmetric states)}, \tag{7a}$$

$$\alpha\cot(\alpha a) = -\beta \quad \text{(antisymmetric states)}. \tag{7b}$$

The solutions to these equations can be determined by graphical[10–14] or numerical techniques.[15–18]

Methods for dealing with multiwell systems[19,20] are less plentiful and considerably more complex. The evaluation of multiple-quantum-well heterostructures involves many finite square wells of different well widths and barrier heights as shown in Fig. 7. In addition, the particle mass can be a function of the bound-state energy or can change as a function of barrier height. The iterative technique presented below can accommodate all of these variations without complicating the basic approach.

The bound-state energies (eigenvalues) and wave functions (eigenvectors) of a system of N coupled wells can be determined by realizing that the resulting wave functions must be well behaved. By "well behaved" we mean that the wave function must be normalizable or, in other words, the wave function must decay exponentially in the semi-infinite (wide-gap) confining layers sandwiching the quantum wells on either side. For simplicity consider a single square well and assume for the moment that the energy E in Eqs. (4), (5), and (6) is an adjustable parameter. If we guess a value of E which corresponds to one of the bound states, say $E = E_1$, then the corresponding wave function is well behaved as shown in Fig. 8. If we guess an energy E which is a little too large or too small then the wave function does not tend to zero asymptotically beyond the wells but di-

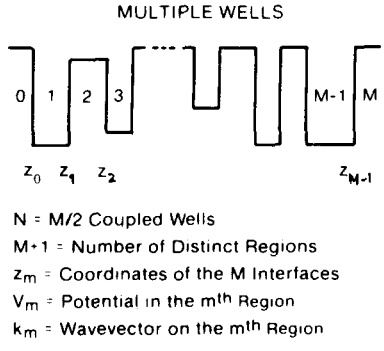

Fig. 7. Multiple finite square wells used as a model to determine the bound-state energies and wave functions by a numerical procedure.

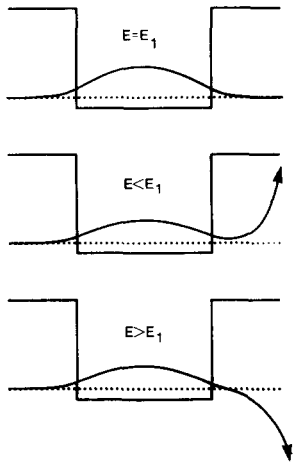

Fig. 8. Ground-state wave function of a finite potential well for the case where the energy E is equal to, less than, and greater than the bound-state energy $E_1 = 38.418$ meV. Note that a correct "guess" of the energy $E = E_1$ produces a well-behaved wave function ($\langle\psi|\psi\rangle$ finite). If too small of an energy ($E = 37$ meV) or too large of an energy ($E = 40$ meV) is guessed or selected, the wave function diverges to plus or minus infinity.

verges to plus or minus infinity as shown in Fig. 8. Thus, the bound-state energies can be determined by finding those energies for which the wave function is well behaved. Plotting the wave function to determine its behavior for many values of E is impractical. However, there are very simple numerical techniques which can provide the required information.

In order to determine the behavior of the wave function as a function of the parameter E, consider the expressions for $\psi(z)$.

$$\psi_j = A_j \cos(k_j z) + B_j \sin(k_j z), \quad E > V,$$
$$\psi_j(z) = A_j \exp(k_j z) + B_j \exp(-k_j z), \quad E < V, \tag{8}$$

where

$$k_j = (2m_j E/\hbar^2)^{1/2}, \quad E > V$$
$$k_j = (2m_j(V-E)/\hbar^2)^{1/2}, \quad E < V. \tag{9}$$

The index j corresponds to the M different regions (layers). For the case of a single finite well, the appropriate expressions for the wave functions in each region are given in Fig. 9. Note that for the choice of $z_0 = 0$ as shown, that B_0 and A_2 must equal zero or ψ diverges to positive or negative infinity. The coefficients A_j and B_j are actually a function of the energy parameter E. If we set $A_0 = 1$ and $B_0 = 0$, then the desired values of E (the E_n's) are determined by

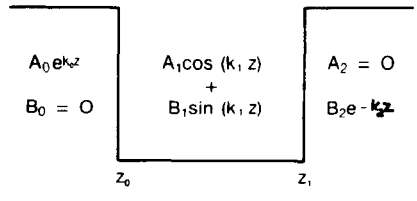

Fig. 9. Analytical expressions for the wave function in the well region and the confining layers of a QWH. Since the wave function must decay exponentially in the confining layers, then the coefficients B_0 and A_2 must be zero.

finding the roots of $A_2(E)$. Thus the problem of solving for the bound-state energies E_n has been reduced to the problem of finding the roots of $A_2(E) = 0$. The coefficient A_2 will be referred to as the coefficient of the unbounded exponential term.

To compute the roots of $A_2(E) = 0$ an expression for $A_2(E)$ is required. First we compute $A_2(E)$ for a single well and then extend the analysis to N wells. Continuity of $\psi(z)$ and $\psi'(z)$ at each well boundary leads to the expression (see Fig. 9),

$$\begin{pmatrix} \exp(k_0 z_0) & \exp(-k_0 z_0) \\ k_0 \exp(k_0 z_0) & -k_0 \exp(-k_0 z_0) \end{pmatrix} \begin{pmatrix} A_0 \\ B_0 \end{pmatrix} = \begin{pmatrix} \cos(k_1 z_0) & \sin(k_1 z_0) \\ -k_1 \sin(k_1 z_0) & k_1 \cos(k_1 z_0) \end{pmatrix} \begin{pmatrix} A_1 \\ B_1 \end{pmatrix}, \tag{10a}$$

at the left boundary z_0 and

$$\begin{pmatrix} \cos(k_1 z_1) & \sin(k_1 z_1) \\ -k_1 \sin(k_1 z_1) & k_1 \cos(k_1 z_1) \end{pmatrix} \begin{pmatrix} A_1 \\ B_1 \end{pmatrix} = \begin{pmatrix} \exp(k_2 z_1) & \exp(-k_2 z_1) \\ k_2 \exp(k_2 z_1) & -k_2 \exp(-k_2 z_1) \end{pmatrix} \begin{pmatrix} A_2 \\ B_2 \end{pmatrix}, \tag{10b}$$

at the right-hand boundary z_1. Thus if we set $A_0 = 1$ and $B_0 = 0$ (required for well-behaved ψ for $z < 0$), then $A_2(E)$ is easily calculated with Eqs. (10a) and (10b). When $A_2(E) = 0$, then E is one of the bound-state energies E_n.

The procedure presented here appears at first quite cumbersome compared to other numerical techniques designed to calculate the bound-state energies of a finite square well. If one considers only a single well, then this approach is much too general and powerful. The power and simplicity of this technique is best appreciated by considering the general case of N coupled wells of varying well widths and depths as shown in Fig. 7. For the case of N wells the continuity of $\psi(z)$ and $\psi'(z)$ at each well boundary leads to $2N$ equations of the form

$$^{j}M_j \begin{pmatrix} A_j \\ B_j \end{pmatrix} = {}^{j}M_{j+1} \begin{pmatrix} A_{j+1} \\ B_{j+1} \end{pmatrix}, \tag{11}$$

where

$$^{m}M_j = \begin{pmatrix} \exp(k_j z_m) & \exp(-k_j z_m) \\ k_j \exp(k_j z_m) & -k_j \exp(-k_j z_m) \end{pmatrix} \quad \text{for } E < V,$$

and

$$^{m}M_j = \begin{pmatrix} \cos(k_j z_m) & \sin(k_j z_m) \\ -k_j \sin(k_j z_m) & k_j \cos(k_j z_m) \end{pmatrix} \quad \text{for } E > V. \tag{12}$$

The coordinates z_m are the positions of the $2N$ layer interfaces, and j is an index for each of the $2N+1$ (or $M+1$) distinct regions as shown in Fig. 7. With the initial conditions $A_0 = 1$ and $B_0 = 0$ it is possible to compute A_j and B_j from the expression

$$\left(\prod_{2N-1}^{0} [\,(^{j}M_{j+1})^{-1} * {}^{j}M_j\,] \right) \begin{pmatrix} A_0 \\ B_0 \end{pmatrix} = \begin{pmatrix} A_{2N} \\ B_{2N} \end{pmatrix} \tag{13}$$

for a set of wave vectors k_j. Since the k_j's and E are related by equations (9), then the solution to the system of equations (11) has been reduced to finding those values of E for which $A_{2N} = 0$.

A plot of the coefficient A_{2N} as a function of E for $N = 1$, 2, 3, and 4 wells is shown in Fig. 10. In this case the well width is 120 Å; the potential depth is 0.106 eV; the spacing between wells is 50 Å. For $N = 1$ (one well) the roots of $A_2(E) = 0$ occur at approximately 20 and 70 meV, which

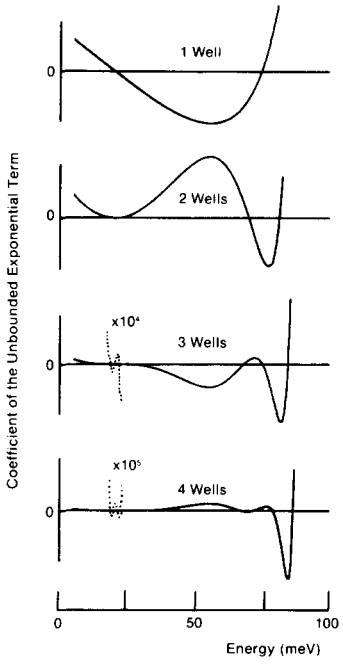

Fig. 10. Plot of the magnitude of A_{2N} (the unbounded exponential term) as a function of energy for the case of $N = 1,2,3$, and 4 wells. A bound state occurs whenever the curve crosses the horizontal energy axis. For the case of one well the two crossings represent the $n = 1$ and $n = 2$ energy levels. For the case of $N = 2$ wells, the four crossings correspond to the symmetric and antisymmetric states of the first two energy levels. As the number of coupled wells increases the number of zero crossings increases simultaneously. These plots have been made for the electron states of 120-Å GaAs wells coupled by 50-Å $Al_x Ga_{1-x}As$ ($x = 0.1$) barriers.

correspond to the $n = 1$ and $n = 2$ bound states. If two wells are coupled ($N = 2$ in Fig. 10), then $A_4(E)$ crosses the horizontal axis twice in the region of 20 meV and twice in the region of 70 meV. The double crossings correspond to the symmetric and antisymmetric (bonding, antibonding) states of the interacting wells. If a third or fourth well is added, then the multiplicity of crossings near the original $n = 1$ and $n = 2$ levels increases accordingly as shown in Fig. 10. (Note that energy splitting of the $n = 2$ level is much greater than the $n = 1$ level.)

The technique presented above is valid for any series of square steps and regions for which Eqs. (8), (9), and (11) and (12) are applicable (e.g., a staircase potential, etc.). Regardless of the number of wells the procedure remains the same. Multiwell structures simply require a series of matrix multiplications to compute $A_{2N}(E)$. The magnitude and sign of $A_{2N}(E)$ varies as E is varied, so that it is possible to design an iterative technique to solve for the roots of $A_{2N}(E) = 0$. For example, if $A_{2N}(E)$ times $A_{2N}(E + \Delta E)$ is negative, then at least one root is located between E and $E + \Delta E$. After a root is isolated it can be identified (i.e., level number, symmetry, etc.) by constructing the wave function from the computed coefficients (A_j's and B_j's) and by counting the number of nodes. This statement is true even for complex multiwell systems and is a consequence of the fact that the kinetic energy is proportional to the curvature of the wave function. Accurate plots of each bound state wave function are readily obtained from Eqs. (8), (9) and the computed coefficients. A sketch of the wave function can be obtained by applying the rules given in Ref. 21.

The procedure outlined here is sufficiently general that multiple wells of variable well widths and depths are easily accommodated. In addition, an energy-dependent particle mass or a change in mass from layer to layer is easily handled.

IV. MULTIPLE QUANTUM WELLS, SUPER LATTICES, AND KRONIG–PENNEY ANALYSIS

The problem of N (N large) interacting wells spaced at equal distances is, of course, well known.[22,23] The outcome of this classic analysis (Kronig and Penney)[22,23] is that each of the single-well levels is split into N closely spaced levels. These closely spaced levels form a nearly continuous band. This type of model has been used traditionally to determine the electron (and hole) energies in solids where the potential has the same period as the atomic lattice. For example, the fundamental band structure (E-k diagram) of bulk GaAs or $Al_x Ga_{1-x}As$ can be determined using this type of model. The energy difference between each band and the energy width of each band depends on the strength of the interaction between each well.

We know that if we couple enough $Al_x Ga_{1-x}As$–GaAs quantum wells (with layer thicknesses greater than 10–20 Å) the problem can be approximated by the Kronig–Penney model. We have already asked and now answer the following question: How many wells are required before the width of the minibands approaches the Kronig–Penney limit? To answer this question we consider 40-Å GaAs wells separated by 40-Å $Al_x Ga_{1-x}As$ barriers with a barrier height of 200 meV (19% Al). The $n = 1$ electron energies for N coupled wells ($N = 1$ to 18) are shown in Fig. 11. The bandwidth as calculated using the Kronig–Penney model is also shown in Fig. 11. Note that the exact solutions rapidly approach the bandwidth predicted by the Kronig–Penney model. In this case only a few (approximately 6 to 10) quantum wells are required before the Kronig–Penney model is applicable. If the interaction between the wells were reduced by increasing the barrier heights or the distance between wells, then additional wells would be required to achieve the same effect.

How many $Al_x Ga_{1-x}As$–GaAs quantum wells are required to form a superlattice? How many Ga and As atoms are required to form the band structure of GaAs? Both of these questions can be considered (zeroth-order approximation) with the techniques presented here. The answers to

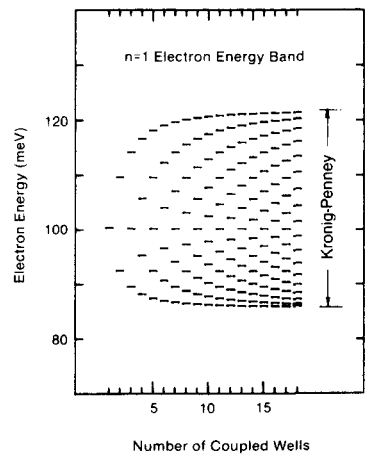

Fig. 11. Electron energy states ($n = 1$) for N coupled wells as a function of the number of identical wells. Note that the width of the "band" rapidly approaches the Kronig–Penney approximation.

these questions depend on the strength of the interaction between the coupled wells. In both cases the interaction is similar to that shown in Fig. 11. Only a few monolayers of Ga and As are required to form GaAs. (The lattice constant of GaAs is 5.6532 Å.) Thus the discussion in Sec. II on GaAs quantum wells is applicable for well widths greater than a few monolayers.

V. CONCLUSIONS

Recent advances in the fabrication of thin semiconductor layers have added a new dimension to both the application and perspective of the traditional discussion of a particle in a box. Quantum notions play a very explicit role in determining the properties of these ultrathin layered structures. Quantum-well heterostructures of $Al_x Ga_{1-x} As$–GaAs are especially interesting, not only as unique optoelectronic device structures, but as an explicit example of a man-made, particle-in-a-box "laboratory."

In Secs. I and II we have presented an introduction and background information on the ideas needed for the elementary (or approximate) modeling of quantum-well heterostructures. Since the finite square well is central to the evaluation of the behavior of quantum wells, it is discussed in detail in Sec. III. A simple iterative technique to calculate the bound-state energies and wave functions of *single and multiple* finite square wells is presented. Nonperiodic multiwell systems are easily evaluated by a series of matrix multiplications. In Sec. IV, we have illustrated the formation of minibands for a large number of identical coupled wells and have compared the exact solutions to the Kronig–Penney model.

ACKNOWLEDGMENTS

The authors are grateful to J. J. Coleman, P. D. Dapkus, and R. D. Dupuis for providing the quantum-well heterostructure crystals used in many of their studies. They wish to thank B. A. Vojak for helpful comments during the early stages of this work and W. D. Laidig for the Kronig–Penney calculations. Some of this work has been supported by the National Science Foundation and the Army Research Office.

APPENDIX

A brief review of solid-state physics terminology is presented. When many atoms are brought together to form a solid, energy bands (essentially continuous bands of energy) evolve from the atomic levels. The highest energy band filled with electrons is called the valence band (VB). The next higher band (empty) is called the conduction band (CB). The "forbidden band" (no allowed energy states) between the valence band and conduction band is called the band gap. The energy separation between the valence and conduction bands is called the band gap energy (E_g). When an electron is promoted from the VB to the CB the empty region left in the VB is called a hole. The concept of a hole is convenient since we can concentrate on the motion of one vacant site rather than the motion of all the electrons remaining in the VB. When an external force is applied to the electrons (or holes) they do not respond as free particles due to the influence of the other atoms. The "effective mass" (m^*) allows us to relate the particle motion to an external force (or potential) without worrying about all the atomic forces. For example, an electron in the CB of GaAs responds as if its mass is $0.0665m_0$ (m_0 = electron mass). A hole in the VB of GaAs can respond as if its mass is $0.45m_0$ (heavy hole) or $0.08m_0$ (light hole).[6]

[1](a) G. Gamow, Z. Phys. **51**, 204 (1928); (b) R. W. Gurney and E. U. Condon, Phys. Rev. **33**, 127 (1929).
[2]H. Faxen and J. Holtsmark, Z. Phys. **45**, 307 (1927). Or see most quantum mechanics textbooks such as E. E. Anderson, *Modern Physics and Quantum Mechanics* (Saunders, Philadelphia, 1971), and L. I. Schiff, *Quantum Mechanics* (McGraw-Hill, New York, 1968).
[3]T. Ando, A. B. Fowler, and F. Stern, Rev. Mod. Phys. **54**, 437 (1982).
[4]Phys. Today **32**, 20 (Search and Discovery section) (1979).
[5]K. Hess and N. Holonyak, Jr., Phys. Today **33**, 40 (1980).
[6]H. C. Casey and M. B. Panish, *Heterostructure Lasers* (Academic, New York, 1978).
[7]R. Dingle, A. C. Gossard, and W. Wiegmann, Phys. Rev. Lett. **34**, 1327 (1975). See also R. Dingle, *Festkorper-problems XV, Advances in Solid State Physics* (Pergamon, New York, 1975), pp. 21–48.
[8]N. Holonyak, Jr., R. M. Kolbas, R. D. Dupuis, and P. D. Dapkus, IEEE J. Quantum Electron. **QE-16**, 170 (1980).
[9]See R. M. Kolbas, "Luminescence Characteristics of Single and Multiple AlGaAs—GaAs Quantum-Well Heterostructure Lasers," Ph. D Thesis, University of Illinois (1979), pp. 21–24 and related references.
[10]Anderson, Ref. 2.
[11]Schiff, Ref. 2.
[12]C. D. Cantrell, Am. J. Phys. **39**, 107 (1971).
[13]A. Messiah, *Quantum Mechanics*, translated by G. Temmer (North-Holland, Amsterdam, 1961), pp. 88–91.
[14]P. G. Guest, Am. J. Phys. **40**, 1175 (1972).
[15]R. D. Murphy and J. M. Phillips, Am. J. Phys. **44**, 574 (1976).
[16]J. D. Memory, Am. J. Phys. **45**, 211 (1977).
[17]S. Garrett, Am. J. Phys. **47**, 195 (1979).
[18]J. R. Merrill and G. P. Hughes, Am. J. Phys. **39**, 1391 (1971).
[19]M. L. Glasser, Am. J. Phys. **47**, 738 (1979).
[20]E. A. Johnson and H. T. Williams, Am. J. Phys. **50**, 239 (1982).
[21]A. P. French and E. Taylor, Am. J. Phys. **39**, 961 (1971).
[22]R. de L. Kronig and W. G. Penney, Proc. Soc. London Ser. A **130**, 499 (1931).
[23]See Refs. 10, 11, or G. C. Wetsel, Jr., Am. J. Phys. **46**, 714 (1978).

PROBLEM

A man whose eyes are at a height h above the floor level and whose trousers' length is l, stands in front of a trial mirror. Show that he should stand at a distance of $\frac{1}{2}[h(h-l)]^{1/2}$ from the mirror in order to get the best view of his trousers. (Solution is on page 464.)